# Bell Inequality Experiment for a High Brightness Time-Energy Entangled Source

Ian R. Nemitz[*a], Jonathan Dietz[b], Evan, J. Katz[a], Brian Vyhnalek[a], Benjamin Child[c,] Bertram M. Floyd[d], and John D. Lekki[a]

[a]NASA Glenn Research Center, 21000 Brookpark Road, Cleveland, OH, USA 44135; [b]Harvard University, 86 Brattle Street, Cambridge, MA, USA 02138; [c]Worcester Polytechnic Institute, 100 Institute Road, Worcester, MA, USA 01609; [d]Sierra Lobo, Inc., 102 Pinnacle Dr., Fremont, OH, USA 43420;

## ABSTRACT

A periodically poled MgO – doped $LiNbO_3$ (MgO:LN) non-degenerate photon pair source is utilized for spontaneous parametric down-conversion of 532 nm photons into time-energy entangled pairs of 794 and 1614 nm photons. The entangled photons are separated using previously detailed sorting optics, such that each wavelength is independently directed through one of two modified Mach-Zehnder interferometers – also known as a Franson interferometer – after which they are fiber-optically guided to high-efficiency photon detectors. Output from the detectors is sent to a high resolution time tagger, where coincidences between the entangled photons are recorded. By varying the length of the long path in one Mach-Zehnder interferometer, it is possible to observe high visibility sinusoidal fringes in the measured coincidence rates (while no variation is seen in single photon detection rates). These fringes – due to interference between the photon probability amplitudes – are indicative of a violation of the Bell inequality, and confirm inconsistencies with local hidden variable theory for the correlations of the time-energy entangled photon pairs.

**Keywords:** Bell inequality, time-energy entanglement, spontaneous parametric down conversion, Franson interferometer, quantum communication

## 1. INTRODUCTION

When Einstein, Podolsky, and Rosen first presented the idea of entanglement - what Einstein dubbed "spooky action at a distance" – it was not to assist in the confirmation of quantum phenomena, but an attempt to refute them[1]. Quantum entanglement describes the non-intuitive physical property that, when two particles are entangled, it is impossible to describe each entangled particle's state without taking into account the state of its partner. This "entangled pair" is tied together such that, if the state of one particle is measured, it is possible to instantaneously know the state of the other, no matter the distance between the two. It was believed – at the time – that this was a violation of locality and realism, and indicated that quantum mechanics was incomplete. This finding (now known as the EPR paradox) was one of the strongest arguments against the non-deterministic nature of quantum mechanics. One logical explanation for this strange property was the presence of local hidden variables – the idea that there is information "stored" in the particles when they are emitted – rather than describing the coupled system as a single wave function.

At the time, there was no clear line of reasoning against the existence of local hidden variables. Nearly thirty years after the EPR paradox had been brought to light, Bell was able to show local hidden variables could not explain a number of statistical predictions made by quantum mechanical theory[2]. He showed that correlation measurements of entangled photon states – such as spin – violated derived inequalities which local hidden variable must satisfy. These violations of "Bell's Inequalities" have been experimentally tested and verified in a number of experiment[3,4], with all possible loopholes recently closed[5].

The usefulness of these entanglement properties lie in their potential applications for optical communication[6,7]. With the advances in quantum computing – and the subsequently decreasing security of classical encryptions protocols – interest is being directed toward increasingly secure communication systems. Unlike their classical counterparts, quantum systems are able to ensure privacy from eavesdroppers by utilizing Heisenberg's uncertainty principle[8] and the "no-cloning" theorem[9]. However, for these new systems to be viable, especially for future aero and space applications, it is necessary to employ single-photon sources that can maintain data rates comparable to today's cutting edge devices, and which are of low size, weight, and power. To meet these requirements, some of the most promising technologies in this vein of research take advantage spontaneous parametric down conversion (SPDC), wherein a single photon (generally generated by a pump laser) is propagated into a bulk nonlinear optical crystal, and spontaneously split into two entangled photons of lower energies.

In this paper we present an analysis of a novel single photon source, developed by AdvR through NASA's SBIR program, which utilized SPDC to generate time-energy entangled photon pairs. Previously, a number of characterization studies have been published on this and similar devices[10,11] and have shown a great deal of promise. In order to confirm that this is truly an entangled single photon source, it was necessary to prove the emitted photons violate Bell's inequality. We report the results of a Bell inequality experiment for a high brightness time-energy entangled source for quantum communication applications, and provide evidence that the studied source produced entangled photon pairs.

## 2. FRANSON INTERFEROMETER

As an alternative to the polarization entanglement used to postulate and prove the existence of entanglement, it is possible to create photons that are time-energy entangled. Photons generated via certain forms of SPDC can be entangled through their time of creation and the conservation of momentum. This is based on the property that the energy of down-converted photons and their relative time of arrival are coupled, via the Heisenberg uncertainty principle for time and energy:

$$\Delta E \Delta T \geq \frac{\hbar}{2} \tag{1}$$

In 1989, Franson proposed a system to measure time-energy entanglement, now known as a Franson interferometer[12]. This system is fundamentally a pair of coupled, spatially-imbalanced Mach-Zehnder interferometers (MZs), used to detect two photon interference in coincident measurements of time-energy entangled photon pairs. By creating a path length difference $\Delta L$ between the MZs long arms and sending entangled photons down each, it is possible to create a time delay $\Delta L/c$ (where $c$ is the speed of light). Varying this time delay (rather than the energy of a photon, which is far more difficult) is equivalent to varying the orientation of the polarizers in more traditional Bell's inequality tests.

The photons in each MZ have two path options (short and long), implying four possible photon coincidence measurements between the two interferometers: short/long (*s*-*l*), long/short (*l*-*s*), short-short(*s*-*s*), and long-long (*l*-*l*).

With proper alignment of both MZs, the *l*-*l* and *s*-*s* processes will be detected at nearly the same time, as those photons will have traveled the same "path" on each interferometer. Because of this, the *l*-*l* and *s*-*s* coincidences become indistinguishable from one another, and it is possible to observe interference between them. When the paths are correctly aligned the coincidences will constructively interfere. When they are completely out of phase with one another, no coincidences will be detected. For this to occur, however, three conditions must be met. First, all single photon interference must be removed. This is done by assuring the difference in length between the MZ short and long paths are significantly larger than the single photon coherence length. Second, the difference in length between the MZ long paths ($\Delta L$) must be less than the two photon correlation length. This imbalance between long arms allows for the observation of the interference, and is based on the temporal coherence of the entangled pair (determined by their individual signal linewidths). Third, the length of both long arms must be within the coherence length of the SPDC source's pump[13].

By incrementally varying $\Delta L$ within the above limitations, it is possible to repeatedly cycle through areas of constructive and destructive interference in coincidence counts. Removing the distinguishable *s*-*l* and *l*-*s* coincidences, and plotting the total indistinguishable *l*-*l* and *s*-*s* coincident counts versus $\Delta L$ allows for the observation of a sinusoidal coincidence fringe pattern. These coincidence fringes represent a violation of Bell's inequality, and are therefore indicative of entanglement.

## 3. EXPERIMENTAL SETUP

### 3.1 Source and Sorting

The single photon source utilized in this experiment was acquired through SBIR with AdvR (Figure 1). The source generates time-energy entangled photons via spontaneous parametric down conversion (SPDC). Light from a 300 mW 1064 nm wavelength stabilized solid state laser diode is filtered through 1064 nm bandpass filter (2nm width) and directed into the waveguide source via single mode (SM) polarization maintaining (PM) fiber. The initial portion of the source up-converts the 1064 nm photons to 532 nm through second harmonic generation (SHG). The 532 nm photons then connect via waveguide to a periodically poled magnesium oxide doped lithium niobate (Mg0:LN) section. Here, approximately one in every billion 532 nm photons is converted into one 794-nm and one 1614-nm photon by means of spontaneous parametric down conversion, and – due to phase matching conditions – the generated photons are entangled in energy and time. The entangled source's output is pigtailed with SM PM 1550 nm fiber that propagated the 794 nm and 1614 nm photons together with the (residual) 1064 nm and 532 nm photons.

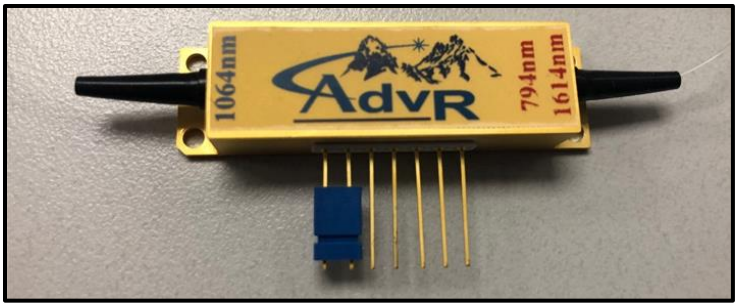


Figure 1 - Image of AdvR source.

Light output from the coupled fiber-optic cable is directed to a series of custom free space sorting optics. The 1064 nm and 532 nm light is removed through a variety of filters, and the 794 nm and 1614 nm photons are efficiently separated using a dichroic mirror. The sorted photons are refocused and directed into separate fiber optic cables, the 794 nm side's output into 50 μm core multimode (MM) fiber and the 1614 nm path's output into 9 μm core PM SM 1550 fiber. More detailed descriptions, as well as system efficiencies, can be found in other published works[10,11].

### 3.2 Interferometer Setup

For the purposes of this study, we constructed a Franson interferometer setup similar to that developed by *Kwiat et al*[13]. Two nearly identical MZs were built – one for each wavelength of interest – using optics coated appropriately for their respective wavelength. Unlike other Franson experiments, fiber optic cabling was used to direct the entangled photons from the source to the interferometers, therefore it was necessary to use fiber-optic coupled collimators to send (receive) photons into (from) their respective interferometers. Adjacent calcite non-polarizing beams splitters (NPBS) were

positioned to split and recombine the photon paths, and retroreflectors were used as means to complete the long arms of each MZ.

The long arms were set to ~ 30 cm (60 cm roundtrip) with the short arms set to ~10 cm. These distances ensured that (i) there was no single photon interference in the measurements, and (ii) the system was aligned within the coherence length of the pump laser (on the order of meters). The retroreflector associated with the 1614 nm MZ was mounted on a nano-stepper motor with 0.5 nm accuracy, while the 794 nm MZ was kept static. The motor is capable of translating the retroreflector ±125 mm. As per the specifications provided by AdvR the linewidths correspond to a window of coherence was the order of 0.5 mm. This implies that, once aligned, the MZ long path length difference ($\Delta L$) needed to be > 0.5 mm to see coincidence interference. The motor was used to assist with the fine adjustments needed to attain this.

Upon exiting the interferometers the photons were returned to the fiber-optic cabling, and measured using single photon detectors. 1614 nm photons were measured using a Quantum Opus superconducting nanowire single photon detector (SNSPD) optimized for detection at 1600 nm, and 794 nm photons were measured using a silicon avalanche photo diode (APD). The detectors were connected to a high speed time tagger set to 100 ps resolution for coincidence counting. The 794 nm photons were treated as idlers and the 1614nm photons as signal. In order to maximize both distinguishable and indistinguishable coincidence counts, both MZ long and short paths were calibrated so that an approximately equal number of photons traveled down each path. A schematic and an image of the setup can be seen in Figure 2(a) and (b) respectively.

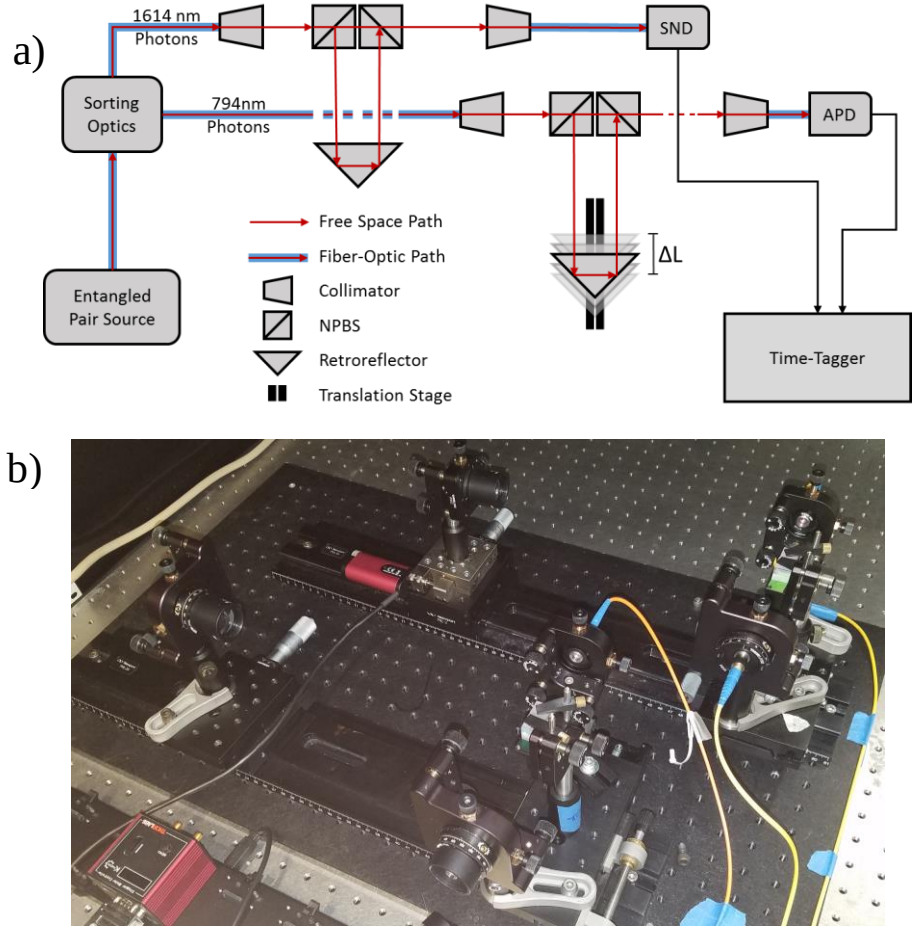


Figure 2 - a) Schematic diagram of the Franson interferometer used in this work b) image of physical setup.

Due to the small length scale where it was possible to observe the desired interference – and to ensure $\Delta L$ was less than 0.5 mm – both gross and fine scans were taken over the maximum range of the stepper motor. Integrating coincidence

counts over 10 s at each point, we scanned up to 5 microns at 10 nm resolution. This was repeated every 50-100 μm, until we were able to identify an area where the indistinguishable coincidence counts began to significantly decrease (indicating destructive interference). At this point the resolution of our scans were reduced to 1 nm, and the integration time was increased to 20 s. Since the movement of the long arm doubles the overall travel distance of the photon, we searched for patterns with a length of 266 nm, half the spatial frequency of the SHG photons. The interferometers were very sensitive to vibrations and external light, so scans were performed in an enclosed environment, absent of extraneous light, air currents, and temperature variations.

## 4. RESULTS AND ANALYSIS

Figure  gives an example of the data acquired for one iteration of the experiment (this particular scan was averaged over 60s). The histogram matches expected results, with the first distinct peak (to the left of the red box) representing *l*-*s* coincidences, the central peak the indistinguishable *s*-*s* and *l*-*l* constructive interference, and the third peak the *s*-*l*. Additional periodic noise proved to be an impedance in determining the total counts, but had minimal effect on the outcome of our results. The program we used to collect data was set to integrate the coincidence counts over 10 bins (1 ns) centered on the central peak (as highlighted by the red box in Figure ). This was done to reject the distinguishable coincidences associated with the *s*-*l* and *l*-*s* peaks during an active scan, rather than through post-processing. The program also subtracted the average background (accidental coincidences and dark counts), and saved all data for analysis.

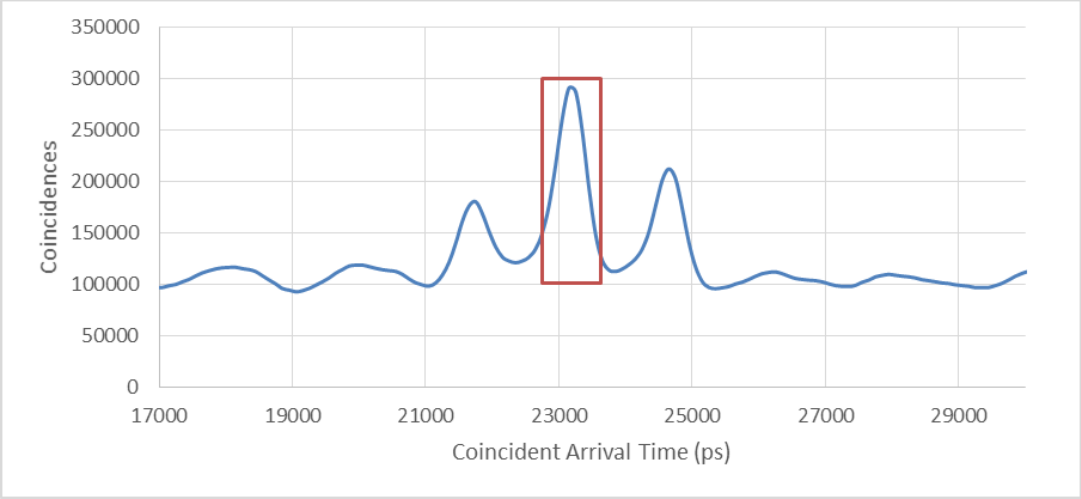


Figure 3 - Histogram coincidence measurements at a single position. Distinguishable processes are rejected by appropriately setting the window of arrival time to integrate over. The data enclosed in red box represent the constructive interference between the *l*-*l* and *s*-*s* coincidences.

The integrated coincidence counts for each position were plotted vs translated distance (as measured by the nano-stepper motor), and were fit to a sinusoid. The fit was performed in order to obtain an estimate of the fringe visibility, from which we were able to observe a maximum visibility of 58.3%, and a fringe spacing of 794 nm (Figure ). Since the set condition for violation of Bell's inequality is a fringe visibility larger than the 50%, this shows that our source is indeed producing time-energy entangled photon pairs. However, this visibility is still relatively low. Increased optical filtering, as well as improved alignment of the system's optics, may be able to increase the fringe visibility. Additionally, the period does not exactly match what is expected from the pump source - which gives an expected fringe period of 532 nm. While this sort of discrepancy is not expected, it has been seen in other work[13]. Factors such as small drifts in the laser frequency over time (the scans can take an hour or more), or imperfections in the nano-stepper motor could account for this.

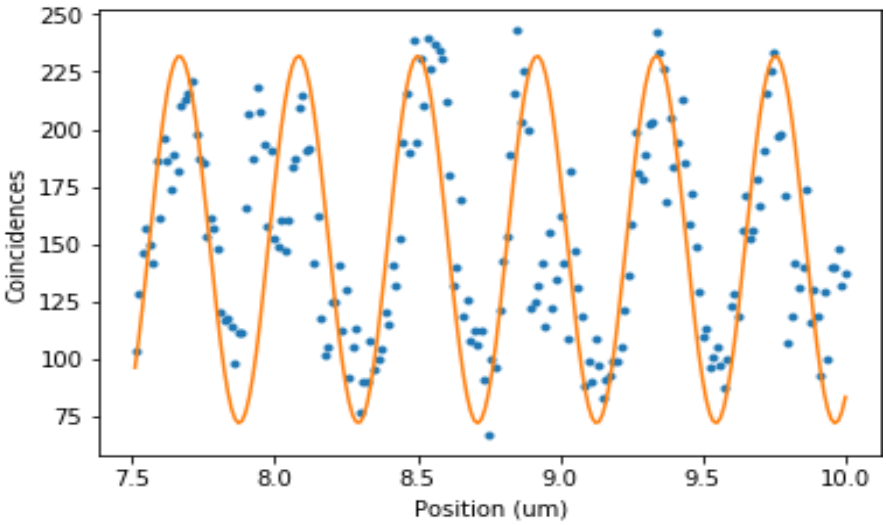


Figure 4 – Sinusoidal fit of coincidences vs translated position. The fringes show a brightness of 58.3%, which indicates a violation of Bell's inequalities, and indicates the generated photons are entangled.

## 5. CONCLUSIONS

In conclusion, we have succeeded in measuring high visibility fringes in a Franson experiment using our periodic poled MgO:LN SPDC waveguide source. We observe a fringe visibility of 58.3%, which exceeds the 50% visibility condition required to violate Bell's inequality, with a period of 794 nm. However, this visibility is still relatively low. Furthermore the period does not match the 532 nm expected from the pump source. Nonetheless, this lays the groundwork for future study of the entanglement properties of our group's high brightness single photon source, and assists in plans to develop aero and space based quantum communication systems around similar devices.

Future entanglement characterization will focus on improvement to visibility and fringe spacing measurements through a number of approaches. Primarily, alignment will need to be examined. Coincident alignment of free-space optics including sensitive orientation of optics – such as beam splitters – have proved challenging, and will be refined so that beams from the long and short paths of both MZs have improved coincidence. Additionally, pinhole apertures may be integrated into the system to clean up the spatial resolution of interfering beams, which would likely reduce noise and increase fringe visibility (though at the loss of total coincidences). Moreover, exchanging the 794 nm output port of the interferometer for a 1.55 um single mode fiber substantial increased visibility, therefore we can expect changing this port further to an 800 nm single mode fiber would likely help even more in increasing visibility – though this would create additional difficulties with alignment. Finally, fringe spacing can likely be remediated by using a motor with less jitter or by using a linear laser rangefinder to monitor the progress of the stage.

## ACKNOWLEDGMENTS

This work is supported by the Advanced Communications project within the NASA Space Communications and Navigation (SCaN) Program.

## REFERENCES

[1] A. Einstein, B. Podolsky and N. Rosen, "Can Quantum-Mechanical Description of Physical Reality be Considered Complete," *Physical Reciew*, vol. 47, no. 10, pp. 777-780, 1935.
[2] J. Bell, "On the Einstein Podolsky Rosen Paradox," *Physics*, vol. 1, no. 3, pp. 195-200, 1964.
[3] S. J. Freedman and J. F. Clauser, "Experimental test of local hidden-variable theories," *Physical Review Letters*, vol. 28, no. 938, pp. 928-941, 1972.

[4] A. Aspect, P. Grangier and G. Roger, "Experimental Tests of Realistic Local Theories via Bell's Theorem," *Physical Review Letters,* vol. 47, no. 7, pp. 460-463, 1981.
[5] B. Hensen, H. Bernien, A. E. Dréau, A. Reiserer, N. Kalb, M. S. Blok, J. Ruitenbert, R. F. L. Vermeulen, R. N. Schouten, C. Abellán, W. Amaya, V. Pruneri, M. W. Mitchell, M. Markham, D. J. Twitchen, D. Elkouss, T. H. Whner and R. Hanson, "Loophole-free Bell inequality violation using electron spins seperated by 1.3 kilometers," *Nature,* vol. 526, pp. 682-686, 2015.
[6] D. Bouwmeester, A. Ekert and A. Zeilinger, The Physics of Quantum Information, New York: Springer, 2001.
[7] A. Ekert, "Quantum cryptography based on Bell's theorem," *Physical Review Letters,* vol. 67, no. 6, pp. 661-663, 1991.
[8] W. Heisenberg, "Uber den anschaulichen Inhalt der quantentheoretischen Kinematik und Mechanik," *Zeitshrift Fur Physik,* vol. 43, no. 3-4, pp. 172-198, 1927.
[9] W. Wooters and W. Zurek, "The no-cloning theorem," *Physics Today,* vol. 62, no. 2, pp. 76-77, 2009.
[10] E. J. Katz, N. C. Wilson, I. R. Nemitz, S. A. Tedder, B. E. Vyhnalek, B. M. Floyd, T. D. Roberts, P. Pandit, S. Baugher, R. P. Tokars, J. J. Pouch and J. D. Lekki, "Coincidence studies of entangled photon paris using nanowire detection and high-resolution time tagging for QKD applications," in *Proc. SPIE 10559, Broadband Access Communication Technologies XII, 1055905*, San Francisco, Ca, 2018.
[11] J. Wilson, D. Chaffee, N. Wilson and J. Lekki, "Free-space quantum key distribution with a high generation rate potassium titanyl phosphate waveguide photon-pair source," *SPIE 9980,* p. 99800U, 2016.
[12] J. D. Franson, "Bell Inequality for Position and Time," *Physical Review Letters,* vol. 62, no. 19, pp. 2205-2208, 1989.
[13] P. G. Kwiat, A. M. Steinberg and R. Y. Chiao, "High-visibility Interference in a Bell-inequality Experiment for Energy and Time," *Physical Review A,* vol. 47, no. 4, pp. R2472-2475, 1993.